OPEN

Citation: Transl Psychiatry (2013) 3, e317; doi:10.1038/tp.2013.92

www.nature.com/tp

ORIGINAL ARTICLE

Latrepirdine is a potent activator of AMP-activated protein kinase and reduces neuronal excitability

P Weisová[1,2,5], SP Alvarez[1,3,5], SM Kilbride[1,5], U Anilkumar[1], B Baumann[1], J Jordán[3], T Bernas[1,4], HJ Huber[1], H Düssmann[1] and JHM Prehn[1]

Latrepirdine/Dimebon is a small-molecule compound with attributed neurocognitive-enhancing activities, which has recently been tested in clinical trials for the treatment of Alzheimer's and Huntington's disease. Latrepirdine has been suggested to be a neuroprotective agent that increases mitochondrial function, however the molecular mechanisms underlying these activities have remained elusive. We here demonstrate that latrepirdine, at (sub)nanomolar concentrations (0.1 nM), activates the energy sensor AMP-activated protein kinase (AMPK). Treatment of primary neurons with latrepirdine increased intracellular ATP levels and glucose transporter 3 translocation to the plasma membrane. Latrepirdine also increased mitochondrial uptake of the voltage-sensitive probe TMRM. Gene silencing of AMPKα or its upstream kinases, LKB1 and CaMKKβ, inhibited this effect. However, studies using the plasma membrane potential indicator $DisBAC_2(3)$ demonstrated that the effects of latrepirdine on TMRM uptake were largely mediated by plasma membrane hyperpolarization, precluding a purely 'mitochondrial' mechanism of action. In line with a stabilizing effect of latrepirdine on plasma membrane potential, pretreatment with latrepirdine reduced spontaneous Ca^{2+} oscillations as well as glutamate-induced Ca^{2+} increases in primary neurons, and protected neurons against glutamate toxicity. In conclusion, our experiments demonstrate that latrepirdine is a potent activator of AMPK, and suggest that one of the main pharmacological activities of latrepirdine is a reduction in neuronal excitability.

Translational Psychiatry (2013) **3,** e317; doi:10.1038/tp.2013.92; published online 22 October 2013

Keywords: AMP-activated protein kinase; bioenergetics; Ca^{2+} homeostasis; glutamate excitotoxicity; mitochondria; plasma membrane potential

INTRODUCTION

Latrepirdine/Dimebon has been safely used as an anti-histaminergic agent for the treatment of allergies and travel diseases in Russia for more than 25 years. Latrepirdine has been shown to improve cognition in rodent models,[1,2] and to enhance memory in rhesus monkeys.[3] Latrepirdine was also successfully tested in a Phase 2 study of patients with mild-to-moderate Alzheimer's disease (AD).[4] The potential mechanisms of latrepirdine's neurocognition-enhancing activities are unrelated to its anti-histaminergic properties, and have been attributed to mitochondria-enhancing or -stabilizing activities.[5,6] However, these apparent 'mitochondrial' activities have been poorly characterized at a molecular level. Despite this shortfall, latrepirdine was subsequently tested in two Phase 3 trials in patients with AD, and in a Phase 2/3 trial in patients with Huntington's disease. All three studies failed to observe any beneficial activity of latrepirdine when studied at a relatively advanced disease stage.[7,8]

Latrepirdine has been suggested to enhance or stabilize mitochondrial membrane potential ($\Delta\psi_m$), an important indicator of mitochondrial function, in primary cortical neurons and human SH-SY5Y neuroblastoma cells.[5] Latrepirdine has also been shown to increase cellular ATP levels, to protect SH-SY5Y cells against serum starvation-induced cell death, and to reduce Ca^{2+}-induced swelling of rat brain mitochondria.[5,9] In the present study, we set out to explore the potential mechanisms underlying the reported mitochondrial activities of latrepirdine. We here describe that latrepirdine is a very potent, small-molecule activator of the intracellular energy sensor, AMP-activated protein kinase (AMPK), acting at low, (sub-) nanomolar concentration ranges. We furthermore demonstrate that the molecular actions of latrepirdine include profound changes on plasma membrane potential and neuronal excitability, and investigate the conditions in which latrepirdine may confer protection against excitotoxic neuronal injury.

MATERIALS AND METHODS

Supplementary Information includes materials and a detailed description of techniques not described in the main text.

Immunofluorescence

As previously described,[10] cerebellar granule neurons (CGNs) were harvested from a 24-well plate using trypsin and fixed in 1% formalin for 20–25 min at 4 °C in the absence of a permeabilization step. Cells were incubated with a rabbit polyclonal GLUT 3 antibody (Millipore Bioscience Research Reagents, Billerica, MA, USA), diluted 1:250 in PBS and 0.1% BSA for 1 h; cells were washed and incubated with an Alexa Fluor 488 goat anti-rabbit IgG (H + _L) antibody (Invitrogen, Biosciences, Dublin, Ireland)

[1]Department of Physiology and Medical Physics, Centre for the Study of Neurological Disorders, Royal College of Surgeons in Ireland, Dublin, Ireland; [2]Max F. Perutz Laboratories, University of Vienna, Vienna, Austria; [3]Dpto Ciencias Médicas-Farmacología, Faculdad de Medicina, Universidad de Castilla-La Mancha, Albacete, Spain and [4]Institute of Experimental Biology PAS, Warsaw, Poland. Correspondence: Professor JHM Prehn, Department of Physiology and Medical Physics, Centre for the Study of Neurological Disorders, Royal College of Surgeons in Ireland, 123 Saint Stephen's Green, Dublin, 2, Ireland.
E-mail: prehn@rcsi.ie
[5]These authors contributed equally to this work.
Received 3 September 2013; accepted 9 September 2013

diluted 1:250 for 1 h. After washing the cells three times with PBS/0.1% BSA, samples were analyzed immediately by flow cytometry on a Partec CyFlow ML (Münster, Germany) followed by analysis using FloMax software. In all cases, a minimum of 10^4 events were acquired.

Preparation of primary CGNs

Murine or rat cerebellum was extracted from postnatal day 7–8 pups and CGNs were prepared as described previously.[11] Briefly, cells were cultured on poly-D-lysine-coated glass Willco dishes (Amsterdam, The Netherlands), 6-well plates and 24-well plates at a density of 1×10^6 cells per ml, or on 96-well plates (Corning) at a density of 50 000 cells per well in 100 μl, and maintained at 37 °C in a humidified atmosphere of 5% CO_2/95% air. Experiments were carried out after 7 days in culture when cells became sensitive to glutamate excitotoxicity. All animal work was carried out with ethics approval from the RCSI Research Ethics Committee and under the licenses obtained from Irish government granted to the authors under the Cruelty to Animal Act, 1976. A record of killed pups was taken down and annual report was submitted to the Irish Department of Health and Children.

Preparation of mouse neocortical neurons

Primary cultures of cortical neurons were prepared from E16 to E18 as described previously.[12] To isolate the cortical neurons, hysterectomies of the uterus of pregnant female mice were performed using an abdominal injection of 40 mg kg^{-1} pentobarbital (Dolethal) as lethal anesthesia. The cerebral cortices were pooled in a dissection medium on ice (PBS with 0.25% glucose and 0.3% bovine serum albumin). The tissue was incubated with 0.25% trypsin–EDTA at 37 °C for 15 min. After the incubation, the trypsinization was stopped by the addition of medium containing sera. The neurons were then dissociated by gentle pipetting, and, after centrifugation (300*g* for 3 min), the medium containing trypsin was aspirated. Neocortical neurons were then resuspended in fresh plating medium (MEM containing 5% fetal calf serum, 5% horse serum, 100 U ml^{-1} penicillin/streptomycin, 0.5 mM L-glutamine and 0.6% D-glucose). Cells were plated at 2×10^5 cells per cm^2 on poly-lysine-coated plates and incubated at 37 °C, 5% CO_2. The plating medium was exchanged with 50% feeding medium (Neurobasal medium embryonic containing 100 U ml^{-1} Pen/Strep, 2% B27 and 0.5 mM L-glutamine) and 50% plating medium with additional cytosine arabinofuranoside (600 nM). After 2 days, the medium was again exchanged for complete feeding medium. All experiments were performed on days *in vitro* 8–11. All animal work was performed with ethics approval and under licenses granted by the Irish Department of Health and Children.

Glutamate toxicity

After 7–8 days in culture, primary neurons were treated with glutamate/glycine at concentrations of 100 μM/10 μM for 10 min in experimental buffer composed of 120 mM NaCl, 3.5 mM KCl, 0.4 mM KH_2PO_4, 5 mM $NaHCO_3$, 20 mM HEPES, 1.2 mM Na_2SO_4 supplemented with glucose (15 mM) and $CaCl_2$ (1.2 mM) at pH 7.4. Cultures were rinsed with 1.2 mM $MgCl_2$-supplemented experimental buffer and returned to preconditioned media.

Determination of neuronal injury

Cells cultured on 24-well plates were stained alive with Hoechst 33258 (Sigma) at a final concentration of 1 μg ml^{-1}. Nuclear morphology was imaged using an Eclipse TE 300 inverted microscope (Nikon) and a ×20 dry objective. For each timepoint and treatment (glutamate/glycine, 100 μM/10 μM; latrepirdine 0.1–100 nM), cells were analyzed for apoptotic morphology in three subfields of each well (1000–2,000 cells per well) in a blinded manner. All experiments were performed at least twice with similar results.

Automated epifluorescence analysis of Hoechst 33258 staining and propidium iodide (PI) uptake using the Cellomics high-content screening platform

To test the effects of a range of concentrations of latrepirdine against glutamate excitotoxicity on a single-cell level, we used a Cellomics ArrayScan VTI platform (Pittsburgh, PA, USA). The platform consists of an automated epifluorescence microscope connected to an automated plate reader with temperature (37 °C) and CO_2 control. CGNs seeded at density 10^5 per well were grown on a 96-well plate for 7 days and either pretreated (for 24 h before glutamate treatment) or co-treated with a range of concentrations of latrepirdine (0.01 nM – 100 nM). For quantification of cell death, neurons were double stained with low concentrations of Hoechst 33258 (100 nM for 1 h before imaging) and PI (150 ng ml^{-1} supplemented in culture media). Apoptotic and necrotic cells were determined based on the intensity of Hoechst staining and nuclear morphology. Hoechst-positive cells with large (or normal) nucleus and PI negative were considered as healthy neurons, Hoechst positive (high intensity) with condensed nuclei were considered as apoptotic and Hoechst and PI positive with large (or normal) were considered as necrotic. A ×10 dry objective was used and nine subfields within each well (5000–6000 cells) were imaged at 60-min intervals over 24 h. Dye concentration and image acquisition rate were optimized to reduce phototoxicity. A 120-W metal halide lamp was for activation of the fluorophores. PI was excited at 545–575 nm; emission was collected through a band pass of 590–625 nm. Hoechst was excited at 381–394 nm and emission light was collected through a 415–460 nm band pass filter. Images were registered using a Hamamatsu Orca AG CCD and digitized at 12-bit precision. Segmentation of cell nuclei was performed on the Hoechst channel using locally adaptative Otsu thresholding, implemented in Cell Profiler (http://www.cellprofiler.org/). Quantification of apoptotic, primary necrotic and healthy cells was executed using a CR&T classifier (validated by a human expert), with nuclear area and fluorescence intensity (Hoechst and PI, average, s.d., min and max) serving as the input.

shRNA and transfection of CGNs

Transfection of CGNs was performed at days *in vitro* 6 using the calcium-phosphate-based transfection method as previously described.[10] Briefly, to produce the DNA/CaP_i coprecipitate, a mixture of $CaCl_2$ solution, distilled H_2O, DNA plasmid solution (equivalent of 3 μg DNA), and 2 × BBS (50 mM BES, pH 7.1 (*N*,*N*-bis[2-hydroxyethyl]-2-aminoethanesulfonic acid, 280 mM NaCl, 1.5 mM Na_2HPO_4) was used. The transfection mixture was added to the transfection medium (pH 7.65) in the culture dish. Cells were incubated in a humidified incubator (without CO_2) at 36.5 °C until the formation of the DNA/CaP_i coprecipitate. The cells were then washed with pre-warmed (36.5 °C) Hank's balanced saline solution (HBSS) washing buffer to ensure that the precipitates have dissolved completely. Finally, cells were incubated in conditioned neuronal tissue culture medium. shRNA targeting *ampk α1/α2* (pFIV-AMPK-shRNA) and scrambled sequence (pFIV-Control-shRNA) were prepared and used as described previously.[10] For inhibition of LKB1 and CaMKKβ, neurons were transfected with a vector (pGFP-V-RS) expressing either a commercial rat shRNA targeting *lkb1* 5′-TGGTGTCTGGATTCTCACTGAAGTCCTGT-3′ (Gene ID 25048, Origene) or *camkkβ* 5′-CCTGGAATCTTCCGACAGCACCAACACAA-3′ (Gene ID 24245, Origene, Rockville, MD, USA). Cells were used for experiments 48 h after transfection. Efficiency of knockdown of AMPK, LKB1 and CaMKKβ was examined by western blotting.

Measurement of ATP

Cells were treated in 24-well plates, the medium was aspirated, 200 μl of hypotonic lysis buffer (Tris acetate buffer, pH 7.75) was added. Samples were immediately stored at −80 °C. ATP measurements were performed using the ENLITEN ATP assay system bioluminescence detection kit (Promega, Southampton, UK) as per the manufacturer's instructions. Luminescence was recorded using a Tecan GENios well plate reader (Männedorf, Switzerland) in luminescence mode. ATP content values were corrected for protein concentration determined using the Pierce BCA micro protein assay kit, and normalized to vehicle-treated control samples. The content of ATP was calculated by a concentration standard curve with ATP levels normalized to protein content in each sample and expressed as a percentage of the control.

Statistics

Data are given as means ± s.e.m. For statistical comparison, one-way analysis of variance between groups and Student-Newman-Keuls *post hoc* test were carried out on SPSS software (SPSS GmbH Software, Munich, Germany). Where the *P*-value was < 0.05, groups were considered to be significantly different.

RESULTS

Pretreatment with (sub)nanomolar concentrations of latrepirdine provides neuroprotection against glutamate excitotoxicity

Excitotoxicity caused by glutamate receptor overactivation has been shown to contribute to neuronal injury and neurodegeneration in both acute and chronic neurodegenerative disorders, including stroke, AD and Huntington's disease.[13–16] To characterize potentially neuroprotective concentrations of latrepirdine against glutamate excitotoxicity in high throughput and at the single-cell level, we employed a Cellomics ArrayScan high-content screening platform. This technique uses automated epifluorescence microscopy and allowed quantification of effects of latrepirdine on neuronal survival over a wide concentration range over time within the same well plate. Because a previous study has reported protective properties of latrepirdine against serum starvation-induced cell death in SHSY-5Y neuroblastoma cells in a pretreatment paradigm,[5] we pretreated CGNs with 0.01–100 nM latrepirdine for 24 h. Latrepirdine was then washed out and neurons exposed to excitotoxicity using a model of glutamate-induced injury that has been extensively characterized in our laboratory.[10–12,17–20] We identified a narrow, (sub)-nanomolar concentration window of around 0.1 nM, in which latrepirdine conferred a protection against glutamate excitotoxicity (Figure 1a).

We next verified the data obtained from the automated high-content screening assay by manually scoring the percentage of pyknotic nuclei. Pretreatment with latrepirdine (0.01, 0.1 and 1 nM) for 24 h resulted in a significant neuroprotection against glutamate excitotoxicity, with the higher concentration of latrepirdine (100 nM) showing no protective activity (Figure 1b), confirming the Cellomics data set. The concentration of latrepirdine that showed most potent attenuation of cell death was 0.1 nM, thus we used

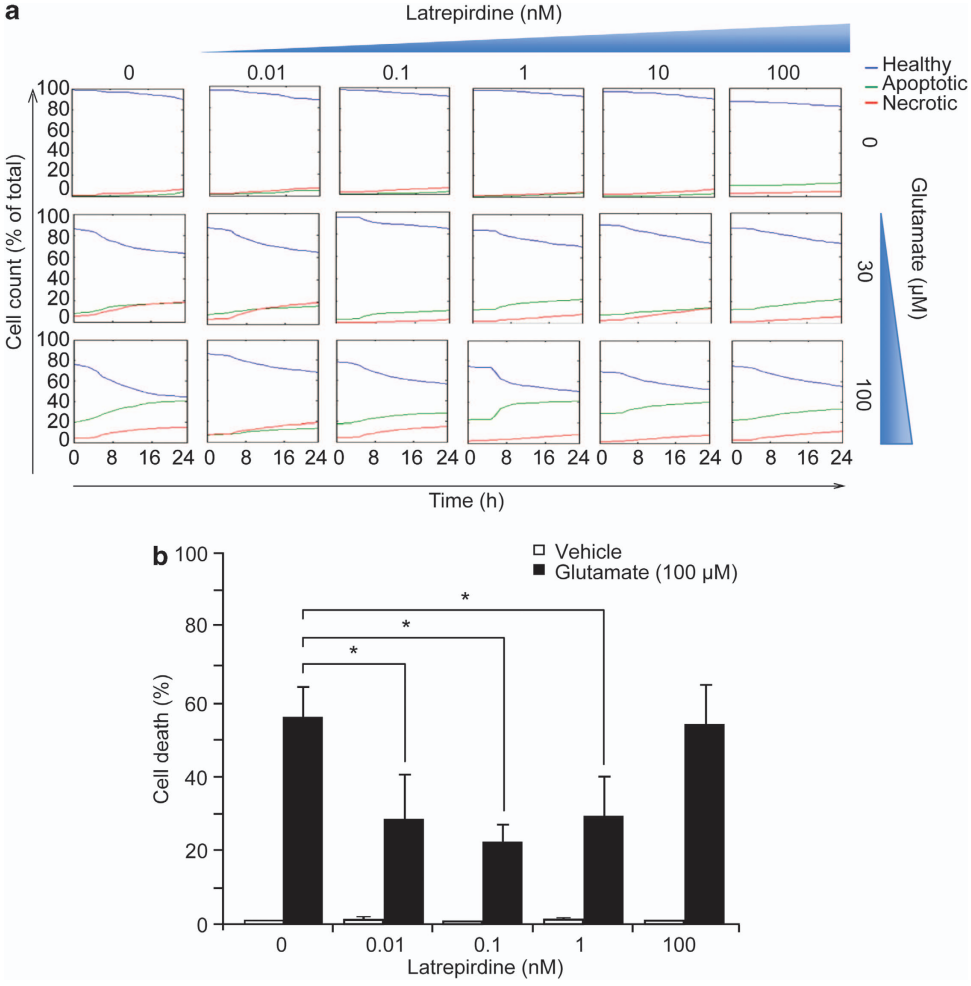

Figure 1. Latrepirdine pretreatment mediates neuroprotection against excitotoxic injury at (sub)nanomolar concentrations. (**a**) High-content time-lapse screening of cell death following glutamate excitation. Murine cerebellar granular neurons plated in a 96-well plate were pretreated with a range of concentrations of latrepirdine (0.01–100 nM) for 24 h as indicated. Cells were stained with Hoechst 1 h before treatment with glutamate/glycine (for 10 min at indicated concentrations) after which cells were washed twice with high Mg^{2+} buffer and preconditioned medium (now containing PI) was replaced. The plate was then immediately placed within the Cellomics imaging chamber (Time 0) and imaged at 1-h intervals over 24 h. Cells were categorized and analysis was carried out using Cell Profiler as described in the Materials and Methods. Data presented are representative traces from thousand of cells, and experiments were carried out on three independent neuronal cultures. (**b**) Murine cerebellar granular neurons were plated in 24-well plates and following pretreatment with latrepirdine (0.01–100 nM as indicated) for 24 h, cells were exposed to glutamate/glycine 100 μM/10 μM for 10 min. After treatment, cells were washed twice with high Mg^{2+} buffer and incubated in preconditioned medium for a further 24 h. Pyknotic nuclei were counted as apoptotic, as determined by Hoechst 33358 staining (1 μg ml^{-1}) and expressed as a percentage of total ($n = 4$ independent experiments in triplicate). Data are presented as mean ± s.e.m. *$P \leqslant 0.001$ indicates difference between glutamate-only treated and latrepirdine (0.01–1 nM)-pretreated glutamate-treated neurons.

this concentration of the compound for all further experiments. Treatment with latrepirdine alone did not affect cell viability at any concentration (Figure 1b). We then examined whether acute treatment with Dimebon exerted any protective activity in the context of glutamate toxicity. Interestingly, acute (10 min) pretreatment with latrepirdine (0.1 nM) failed to provide any neuroprotection against glutamate excitoxicity (Supplementary Figure 1). Collectively, these data suggest that Dimebon can act as neuroprotectant against glutamate excitotoxicity when applied at nanomolar concentrations and in a pretreatment paradigm, however fails to provide any neuroprotection when added concomitantly to excitotoxic stress.

Latrepirdine increases mitochondrial TMRM uptake

In light of previous findings that linked neuroprotective and neurocognitive effects of latrepirdine to improved mitochondrial bioenergetics,[5,9,21,22] we next explored whether the protective effects of latrepirdine pretreatment against glutamate toxicity were related to changes in mitochondrial membrane potential ($\Delta\psi_m$), an indicator of mitochondrial bioenergetics. Neurons were imaged by time-lapse confocal microscopy using the lipophilic, cationic probe TMRM (10 nM) that is taken up into negatively charged mitochondria, following Nernstian behavior, and is thus also sensitive to changes in plasma membrane potential.[17,23] TMRM uptake in single cells can be followed by time-lapse microscopy and under non-quench conditions an increase in fluorescence intensity is indicative of increased uptake.[17] Latrepirdine increased mitochondrial TMRM fluorescence intensity significantly after 60 min (Figures 2a and b), in accordance with data previously obtained in cortical neurons and SH-SY5Y cells.[5] However, there was no difference in TMRM fluorescence intensity during exposure to glutamate when compared to untreated neurons (Supplementary Figure 2), suggesting that glutamate-induced membrane potential depolarization is not affected by latrepirdine.

We next conducted a series of experiments to explore whether the increase in TMRM uptake in response to latrepirdine was solely due to changes in membrane potentials, or partially due to an increase in mitochondrial mass or biogenesis. Neither the expression level of the mitochondrial protein cytochrome *c* oxidase subunit IV (COX IV) nor the total cellular fluorescence intensity of MitoTracker Green, a dye that is taken by mitochondria independently of $\Delta\psi_m$,[24] were altered in neurons treated with latrepirdine (0.1 nM) for 24 h (Supplementary Figures 3 A and B). This suggested that increased mitochondrial mass was not contributing to the increase in TMRM uptake in response to latrepirdine. Furthermore, the mRNA levels of two transcription factors involved in mitochondrial biogenesis, the mitochondrial transcription factor A (*tfam*) and peroxisome proliferator-activated receptor γ coactivator 1α (*pgc-1α*), also remained unaltered in CGN cultures treated for 24 h with latrepirdine (Supplementary Figure 3C).

Latrepirdine hyperpolarizes the plasma membrane potential ($\Delta\psi_p$)

As well as responding to changes in mitochondrial membrane potential ($\Delta\psi_m$), TMRM fluorescence intensity is also affected by changes in plasma membrane potential ($\Delta\psi_p$).[11,17,23,25] To examine a possible contribution of plasma membrane potential ($\Delta\psi_p$) changes to the increase in TMRM uptake, CGNs were loaded with the anionic, $\Delta\psi_p$-sensitive probe $DisBAC_2(3)$ that is extruded from cells upon $\Delta\psi_p$ hyperpolarization.[26] Interestingly, treatment with latrepirdine (0.1 nM) induced a significant decrease in $DisBAC_2(3)$ fluorescence intensity, indicative of $\Delta\psi_p$ hyperpolarization (Figures 2c and d). Quantification of $DisBAC_2(3)$ fluorescence intensities indicated a significant decrease after 90 min of latrepirdine exposure, and decreasing further up to 240 min after drug addition (Figure 2e). These results indicated that the increase in TMRM fluorescence intensity in response to latrepirdine (0.1 nM) may be attributable not only to changes in mitochondrial ($\Delta\psi_m$) but also to changes in plasma membrane potential ($\Delta\psi_p$).

To elucidate more precisely the contribution of plasma membrane potential changes to the TMRM signal kinetics, we fed $\Delta\psi_p$ changes, calculated from average $DisBAC_2(3)$ fluorescence intensity changes (Figure 2f), into a modified Nernstian equation as described in Supplementary Materials (see also Ward *et al.*[17]). The resulting trace is shown in Figure 2g. This approach allowed us to correct TMRM kinetics for changes in $\Delta\psi_p$ kinetics (Figure 2h). This analysis showed that the increase in TMRM fluorescence intensity following treatment with latrepirdine was indeed attributable to changes in $\Delta\psi_p$ (Figure 2f).

Latrepirdine activates AMPK and affects neuronal bioenergetics

We have previously detected a direct link between increased TMRM uptake, pre-conditioning, and activation of an evolutionarily conserved metabolic sensor, AMPK.[10,27,28] Moreover, a recent study has demonstrated that AMPK activation leads to plasma membrane hyperpolarization through phosphorylation of a voltage-sensitive potassium channel.[29] We therefore set out to

Figure 2. Latrepirdine increases TMRM fluorescence intensity and hyperpolarizes $\Delta\psi_p$. (**a**) Representative single-cell traces of changes in TMRM fluorescence intensity following latrepirdine treatment. Latrepirdine (0.1 nM) was added to cells on the confocal microscope stage and TMRM fluorescence intensity was imaged at 5-min intervals over 240 min. Analysis was carried out using Metamorph software and average pixel intensity per cell at each timepoint is shown. (**b**) Quantification of average TMRM fluorescence intensity per cell at selected time points, represented as mean ± s.e.m. *$P \leqslant 0.05$, indicates the difference between 0 min and 60, 120, 240 min after latrepirdine addition ($n = 65$ cells). This experiment was carried out on three independent cultures with similar results obtained. (**c**) Representative images of CGNs loaded with $DisBAC_2(3)$ (1 μM) and treated with latrepirdine (0.1 nM) on a confocal microscope stage showing decreased fluorescence intensity after 210 min. $DisBAC_2(3)$ is a bis-barbituric acid oxonol compound that is incorporated into the plasma membrane as a function of $\Delta\psi_p$. Plasma membrane hyperpolarization is characterized as an extrusion of the probe with subsequent decrease in fluorescence, whereas depolarization results in increased fluorescence. Scale bar, 10 μm. (**d**) The $DisBAC_2(3)$ traces from 105 cells treated with latrepirdine (0.1 nM) were averaged. Neurons were treated with latrepirdine (0.1 nM) at 0 min and fluorescence intensity imaged at 2-min intervals over 240 min. Image analysis was carried out as described in Supplementary Information. (**e**) Quantification of $DisBAC_2(3)$ (1 μM) fluorescence intensity (fl. int.) in vehicle-treated versus latrepirdine (0.1 nM) treated CGNs from selected time points. Average $DisBAC_2(3)$ fluorescence intensity is represented as mean ± s.e.m. *$P \leqslant 0.001$, difference between vehicle-treated and latrepirdine-treated (0.1 nM) neurons stained with $DisBAC_2(3)$ ($n = 105$ cells). This experiment was carried out on three independent cultures with similar results obtained. (**f**) The corresponding $\Delta\psi_p$ values (in mV) for each timepoint in the mean $DisBAC_2(3)$ traces were calculated as described in the Materials and Methods. (**g**) TMRM fluorescence intensity i) reaches a stable baseline when the dye equilibrates across plasma and mitochondrial membranes and increased fluorescence intensity corresponds to increased uptake driven by either ii) plasma membrane potential ($\Delta\psi_p$) hyperpolarization or iii) mitochondrial membrane potential ($\Delta\psi_m$) hyperpolarization. (**h**) The kinetics of the mean TMRM intensity caused by changes in $\Delta\psi_p$ were calculated according to the Nernstian equilibrium of the TMRM concentrations in the buffer, cytosol and mitochondria (see Materials and Methods for equations). Thereby, it was calculated that the measured TMRM kinetics (blue line) indicated that there was a slight latrepirdine-induced depolarization of the $\Delta\psi_m$ (−1.6% at 240 min), as the TMRM signal is lower than the expected increase due to the change in cytosolic TMRM after the $\Delta\psi_p$ hyperpolarization.

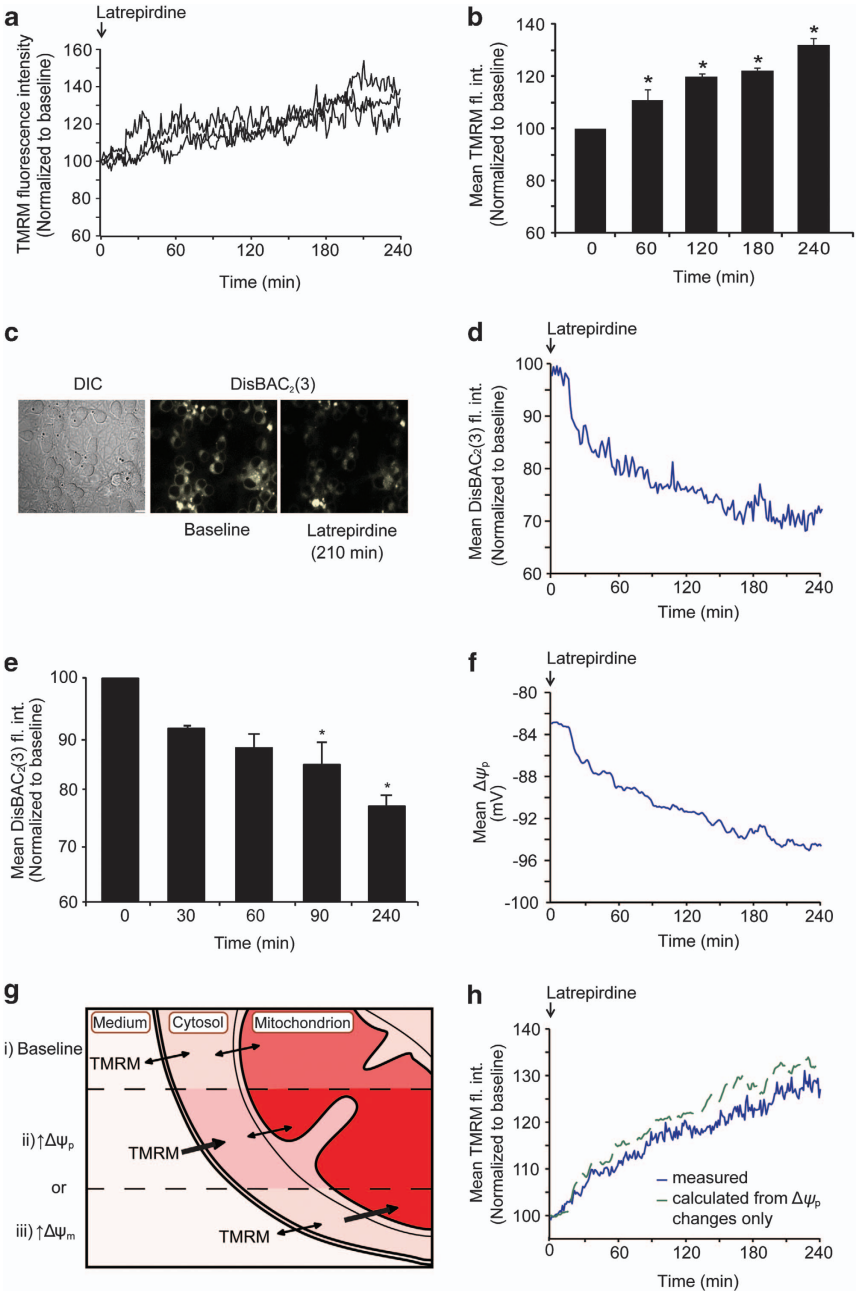

examine whether latrepirdine had a direct effect on the activity of AMPK. Indeed, treatment of CGN cultures with latrepirdine increased the levels of phospho AMPK (Thr 172), indicative of elevated AMPK activity (Figures 3a and b).

Previous studies have identified enhanced glucose transporter 3 (GLUT 3) plasma membrane localization and elevated ATP levels in response to AMPK activation in neurons.[10,27] Therefore, we tested whether latrepirdine treatment altered GLUT 3 translocation in CGNs by examining GLUT 3 cell surface expression. Treatment of neurons with latrepirdine (0.1 nM) led to a significant increase GLUT 3 translocation as evidenced by immunofluorescence and flow cytometry analysis (Figures 3c and d). We also detected a significant increase in neuronal ATP levels after 24-h latrepirdine treatment (Figure 3e), suggesting that Dimebon-induced AMPK activation may enhance neuronal bioenergetic function or decrease ATP utilization.

Latrepirdine-induced hyperpolarization of $\Delta\psi_p$ requires AMPK and its upstream kinases LKB1 and CaMKKβ

To assess whether increased AMPK signaling directly mediated latrepirdine-induced changes in cellular physiology, we employed small hairpin RNA (shRNA) technology to suppress AMPKα expression 24 h before latrepirdine treatment as reported previously (Figure 4a).[10] Experiments were conducted using TMRM uptake as read-out, and were evaluated on the single-cell level as the shRNA contructs co-expressed GFP. Live-cell confocal imaging microscopy of neurons with suppressed AMPKα (*AMPKα shRNA*) revealed a complete suppression of latrepirdine-induced alterations in TMRM uptake when compared with control shRNA-transfected neurons (Figures 4b and c). Changes in $DisBAC_2(3)$ fluorescence intensity were also reduced in *AMPKα* shRNA-transfected neurons (Figure 4d). We then addressed the question as to whether the upstream AMPK kinases (AMPKK), LKB1 and

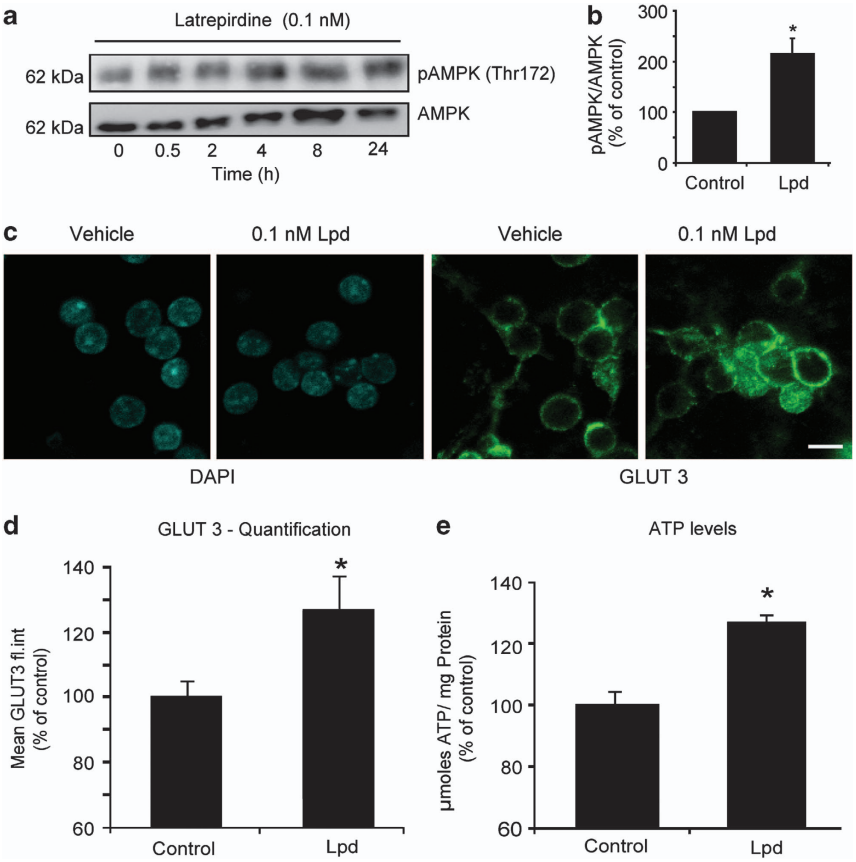

Figure 3. Latrepirdine induces AMPK activation and GLUT 3 translocation and increases ATP levels. (**a**) CGNs were treated with latrepirdine (0.1 nM) and were lysed for protein quantification at indicated time points. The level of phosphorylated AMPK (Thr 172) relative to the total level of AMPK, which corresponds to activation status of the enzyme, was examined by western blotting and (**b**) quantified using Image J (at 24-h timepoint post latrepirdine administration). This experiment was repeated three times with similar results. (**c**) Representative immunofluorescence images of plasma membrane localization of GLUT 3 in vehicle and latrepirdine (0.1 nM)-treated neurons. Scale bar, 10 µm. (**d**) Quantification of GLUT 3 plasma membrane localization in vehicle and latrepirdine (0.1 nM)-treated CGNs by immunofluorescence by flow cytometry. The mean fluorescence intensity of each population was obtained, and data are presented as mean ± s.e.m. of $n = 3$ populations. *$P \leqslant 0.001$ indicates difference between vehicle versus latrepirdine-treated neurons. This experiment was done in triplicate from 3 independent cultures. (**e**) CGNs were treated with latrepirdine (0.1 nM for 24 h), lysed and intracellular ATP content was determined as described in Materials and Methods. Data are shown as mean ± s.e.m. and the experiment was repeated on three independent preparations. *$P \leqslant 0.01$ indicates difference between vehicle versus latrepirdine-treated neurons.

CaMKKβ[30–32] could modulate the latrepirdine-induced changes in TMRM uptake. Transfection of neurons with shRNA plasmids targeting LKB1 (*LKB1 shRNA*) or CaMKKβ (*CaMKKβ shRNA*) also led to a significant depletion of neuronal LKB1 and CaMKKβ levels (Figure 4a). Gene silencing of either *LKB1* or *CaMKKβ* prevented neuronal TMRM uptake in latrepirdine-treated neurons, suggesting that the activity of both kinases was required for the latrepirdine-induced increase in plasma membrane potential (Figures 4b and c). We also pharmacologically inhibited AMPK using the small-molecule inhibitor Compound C.[10,12,33,34] Treatment with Compound C (10 µM) prevented the latrepirdine-induced changes in $DisBAC_2(3)$ and TMRM (Figures 4e and f). Collectively, these results suggested that the latrepirdine-induced hyperpolarization of the plasma membrane potential required AMPK.

Pretreatment with latrepirdine attenuates cytosolic Ca^{2+} influx during glutamate excitation and decreases spontaneous Ca^{2+} elevations in neurons

Glutamate excitotoxicity is characterized by excessive Ca^{2+} influx through NMDA receptors, leading to intracellular Ca^{2+} overload.[35] Indeed, glutamate-induced Ca^{2+} elevations critically depend both on the magnitude of plasma membrane potential depolarization,[36] as well as ATP-dependent Ca^{2+} extrusion.[37] Our observations of plasma membrane hyperpolarization and the changes in cellular bioenergetics in response to latrepirdine posed the question whether protection by pretreatment with latrepirdine may be mediated by reduced neuronal Ca^{2+} overloading during glutamate excitation. CGN neurons were pretreated with latrepirdine (0.1 nM), and changes in cytosolic Ca^{2+} levels were monitored by confocal microscopy using Fluo-4 A.M. CGNs pretreated for 24 h with latrepirdine, and then exposed to glutamate and glycine (100 µM/10 µM for 10 min) significantly attenuated cytosolic Ca^{2+} influx (Figures 5a and b). Quantification of peak fluo-4 fluorescence (Figure 5b) during the glutamate exposure showed a robust attenuation of Ca^{2+} influx in CGN neurons pretreated with latrepirdine (0.1 nM) for 24 h compared with vehicle-pretreated neurons. This finding was furthermore confirmed by the observation that pharmacological activation of AMPK with AICAR (0.1 mM, 24 h before glutamate excitation) also led to a significant attenuation of cytosolic Ca^{2+} levels during NMDA receptor overactivation in cortical neurons (NMDA alone: 5516.72 ± 1126.52 fl. int. units, $n = 70$ cells vs. AICAR pretreated 3174.34 ± 1152.78 fluorescence intensity units, $n = 67$ cells, $P < 0.001$). Collectively, these data suggested that pharmacological

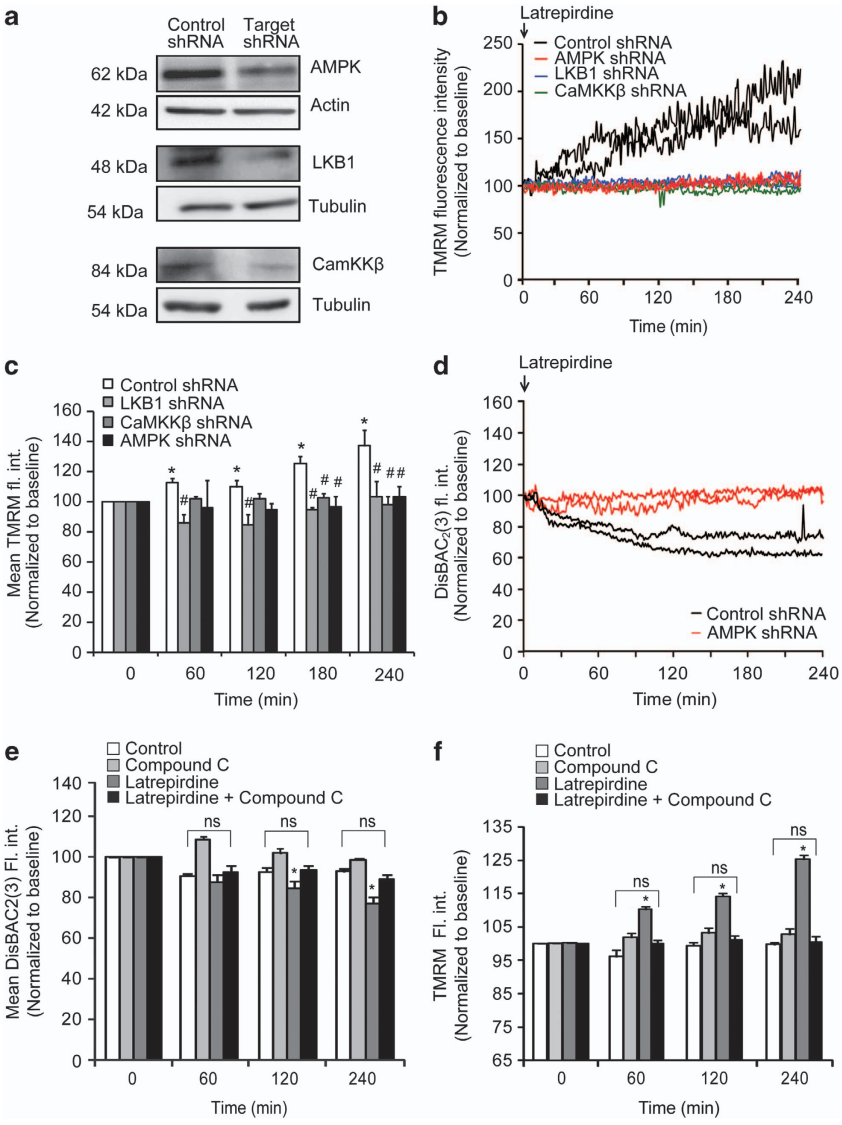

Figure 4. Inhibition of either AMPK activation or its upstream kinases (LKB1 and CaMKKβ) abolishes the latrepirdine-induced increase in TMRM fluorescence/decrease in $DisBAC_2(3)$. (**a**) Western blot analysis of CGNs transfected with short hairpin RNA (shRNA) directed against AMPK α1/α2, LKB1 or CaMKKβ versus a non-targeting shRNA (control shRNA) in respective experiments. Actin or tubulin served as loading controls. The blots shown are representative of three independent experiments. (**b**) Representative single-cell traces of changes in TMRM (10 nM) fluorescence intensity following latrepirdine treatment of neurons transfected with control shRNA, AMPKα shRNA, Lkb1 shRNA and CamkB shRNA. Analysis was carried out using Metamorph software and average pixel intensity per cell at each timepoint is shown. Only transfected, GFP-positive neurons were included in the analysis. (**c**) Quantification of TMRM fluorescence at indicated time points (60, 120, 180 and 240 min) post latrepirdine (0.1 nM) addition for neurons transfected with control shRNA ($n = 86$ cells), AMPKα shRNA ($n = 47$ cells), LKB1 shRNA ($n = 60$ cells) and CaMKKβ shRNA ($n = 61$ cells). Data are shown as mean ± s.e.m. $^*P < 0.001$ indicates difference between control shRNA in timepoint 0 min versus later time points after latrepirdine addition (60, 120, 180 and 240 min). $^{\#}P < 0.001$ indicates difference between control shRNA neurons treated with latrepirdine (0.1 nM) versus neurons transfected with shRNAs directed against AMPK, LKB1 and CaMKKβ treated with latrepirdine. (**d**) Representative single-cell traces of changes in $DisBAC_2(3)$ (preincubated at 1 μM for 30 min at 37 °C) fluorescence intensity following latrepirdine addition (0.1 nM) in neurons transfected with AMPK shRNA versus control shRNA. Analysis was carried out using Metamorph software and average pixel intensity per cell at each timepoint is shown. Fluorescence intensity is represented as mean ± s.e.m. $^*P \leqslant 0.001$ compared with group pretreated with vehicle. (**e**) Quantification of $DisBAC_2(3)$ (1 μM) fluorescence intensity (fl. int.) in vehicle-treated (control) versus latrepirdine (0.1 nM)-treated CGNs from selected time points. Average $DisBAC_2(3)$ fluorescence intensity is represented as mean ± s.e.m. $^*P \leqslant 0.001$, difference between control-treated and latrepirdine-treated (0.1 nM) neurons stained with $DisBAC_2(3)$ ($n = 78$ cells). Effect of latrepirdine was abolished in neurons with inhibited AMPK activity (Compound C pretreatment 10 μM) marked as ns. (**f**) Quantification of TMRM fluorescence at indicated time points (0, 60, 120 and 240 min). Neurons were pretreated with either vehicle (control) or latrepirdine (0.1 nM) ± AMPK inhibitor Compound C (10 μM). Data are shown as mean ± s.e.m. $^*P < 0.01$ indicates difference between control and latrepirdine-treated neurons. This significance was abolished in neurons with inhibited AMPK activity (Compound C + latrepirdine) marked as ns.

AMPK activation with latrepirdine pretreatment affects Ca^{2+} handling in primary neurons in response to glutamate excitotoxicity. Interestingly, acute pretreatment with latrepirdine (0.1 nM, 10 min before glutamate) did not attenuate Ca^{2+} influx (Supplementary Figures 4A and B), suggesting that latrepirdine did not act directly on glutamate receptors.

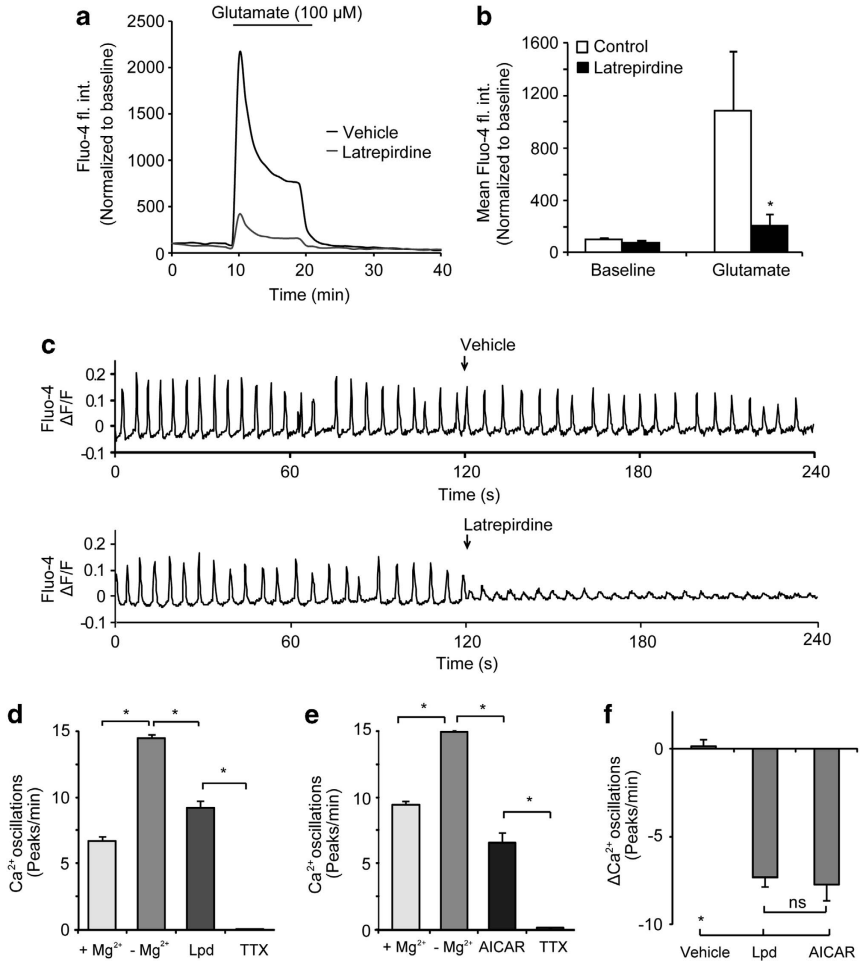

Figure 5. Latrepirdine pretretment attenuates the increase in cytosolic Ca^{2+} during glutamate excitation and reduces spontaneous Ca^{2+} oscillations. (**a**) Average single-cell traces of changes in fluorescence intensity of the cytosolic Ca^{2+} indicator Fluo-4 AM in response to glutamate excitation. CGNs pretreated with latrepirdine (0.1 nM for 24 h were loaded with Fluo-4 AM (3 μM) and mounted on the confocal microscope stage. Glutamate excitation (glutamate/glycine [100 μM/10 μM] for 10 min immediately followed by addition of MK 801 [2.5 μM]) was induced as indicated. Analysis was carried out using Metamorph software and average pixel intensity per population at each timepoint is shown. (**b**) Quantification of area under the Fluo-4 AM curve during glutamate excitation in prolonged latrepirdine-pretreated neurons. Vehicle: $n = 30$ cells; latrepirdine: ($n = 45$ cells). Data are shown as mean ± s.e.m. $^*P < 0.001$ compared with vehicle-pretreated neurons that were glutamate treated. (**c**) Murine cortical neurons were cultivated on glass bottom dishes, incubated with 5 μM Fluo-4-AM for 45 min at 37 °C, washed, perfused with experimental buffer supplemented with 2 mM $MgCl_2$ and placed on the heated stage of a LSM 5live microscope. Images were taken at 5 Hz, optical slice thickness set to 3.5 μm. The buffer was replaced with $MgCl_2$-free buffer at time 0 and either vehicle or latrepirdine (0.1 nM) was added after 120 s of imaging as indicated. Typical Fluo-4 kinetics are shown as change in fluorescence intensity divided by the mean overall fluorescence intensity ($\Delta F/F$). (**d**) Quantification of Ca^{2+} spike frequency after $MgCl_2$ washout, treatment with latrepirdine (0.1 nM, $n = 176$ cells) or (**e**) AICAR (0.1 mM) ($n = 88$ cells) addition followed by complete block using tetrodotoxin (TTX, 1 μM) (significant difference $P < 0.05$, paired *t*-test). (**f**) Quantification of changes of the Ca^{2+}-spiking activity due to addition of latrepirdine, AICAR, or vehicle (Control, $n = 134$ cells, latrepirdine, $n = 176$ cells, AICAR $n = 88$ cells, Kruskal–Wallis and subsequent Mann–Whitney tests showed a significant difference in latrepirdine and AICAR compared with control (*) but no significant difference in latrepirdine compared with AICAR (ns).

Having observed that latrepirdine activates AMPK and also hyperpolarizes neuronal plasma membrane potential, we next turned our attention to the effects of latrepirdine on neuronal excitability, which was recently shown to be directly regulated by AMPK activity.[29] To address this, we measured spontaneous Ca^{2+} oscillations in single-cortical neurons using high-frequency time-lapse confocal microscopy. The addition of 0.1 nM latrepirdine caused a significant attenuation of spontaneous Ca^{2+} spiking in the absence of Mg^{2+} compared to vehicle (Figure 5c). Quantification of the effect of latrepirdine showed an average reduction of spiking frequency from 14.0 ± 0.3 to $8.9 \pm 0.5\ min^{-1}$ (Figure 5d) The frequency of spiking was significantly lower in the presence of Mg^{2+} (2 mM), and addition of Tetrodotoxin (TTX, 1 μM) completely abolished spontaneous Ca^{2+} spiking (Figure 5d). In accordance with previous evidence indicating that activation of AMPK reduces neuronal excitability,[29] acute exposure of the cells to the AMPK activator AICAR (0.1 mM) reduced the Ca^{2+}-spiking frequency from 13.8 ± 0.1 to $6.1 \pm 0.7\ min^{-1}$ (Figure 5e). Direct comparison of changes in frequency of oscillations induced by each compound revealed that 0.1 nM latrepirdine reduced neuronal excitability as potently as 0.1 mM AICAR, as no significant difference was found between the two groups (Figure 5f).

DISCUSSION

Most of the current therapeutic strategies for the treatment of AD are designed to target NMDA receptor overactivation, or to target β amyloid itself by interfering with its synthesis, aggregation or

degradation. Latrepirdine has gained significant interest as a novel class of therapeutic agents that target 'mitochondria', but has subsequently failed in clinical trials. We here demonstrate that latrepirdine is an activator of the energy sensor, AMPK, acting at surprisingly low, (sub-) nanomolar concentrations. We furthermore describe that the pharmacological activities of latrepirdine in primary neuron cultures include a pronounced effect on $\Delta\psi_p$, and a strong inhibitory effect on neuronal excitability and glutamate-induced Ca^{2+} increases.

During conditions of increased energy demand, AMPK is activated as a protective response in an attempt to restore cellular homeostasis.[28] Our findings that latrepirdine activates AMPK is in agreement with previous studies that demonstrated that latrepirdine improves neuronal energy metabolism[38] and mitochondrial function.[5,22] Supporting these findings, we demonstrate that latrepirdine triggers an increase in GLUT 3 translocation that was coupled with an increase in neuronal ATP levels. Latrepirdine has previously been shown to enhance cerebral glucose utilization in aged mice *in vivo*.[39] We also observed that latrepirdine treatment led to a pronounced increase in mitochondrial uptake of the cationic dye, TMRM, suggestive of $\Delta\psi_m$ hyperpolarization.[17] This effect was abrogated in neurons in which AMPKα expression was silenced, demonstrating the requirement of AMPK for the effect of latrepirdine on mitochondrial TMRM uptake. However, TMRM uptake into cells is determined by the Nernst potential across both plasma and mitochondrial membranes.[11,25] Subsequent experiments indicated that latrepirdine also induced a strong $\Delta\psi_p$ hyperpolarization. It is important to mention in this context that AMPK has previously been shown to hyperpolarize $\Delta\psi_p$ through the phosphorylation of a voltage-sensitive potassium channel.[29] Indeed, further quantitative analysis demonstrated that $\Delta\psi_p$ hyperpolarization largely contributed to the latrepirdine-induced increased in TMRM uptake, precluding a pure 'mitochondrial' action of latrepirdine. As the plasma membrane Na^+/K^+ ATPase uses at least 50% of neuronal ATP to maintain resting $\Delta\psi_p$,[40] a $\Delta\psi_p$ hyperpolarization may also indirectly preserve cytosolic ATP expenditure, and thus may contribute to the increase in cellular ATP levels in response to latrepirdine treatment as observed in this and previous studies.

Our study also demonstrated that treatment with latrepirdine reduced glutamate-induced and 'spontaneous' cytosolic Ca^{2+} elevations, indicating that the latrepirdine-induced hyperpolarization of $\Delta\psi_p$ correlated with decreased neuronal excitability. We noted a strong inhibition of glutamate-induced Ca^{2+} elevations following latrepirdine pretreatment, but not during acute treatment, suggesting that latrepirdine does not directly inhibit NMDA or other glutamate receptors. The inhibitory effect of latrepirdine pretreatment on glutamate-induced Ca^{2+} elevations could be due to plasma membrane potential hyperpolarization limiting NMDA receptor activation, or due to an improvement of neuronal ATP levels, enabling a faster removal of cytosolic Ca^{2+} via plasma membrane ATPases or the Na^+/K^+-ATPase-driven Na^+/Ca^{2+} exchanger. It is also possible that latrepirdine pretreatment alters NMDA receptor function or expression, however this requires further detailed investigation. We also found that latrepirdine potently reduced spontaneous Ca^{2+} spiking in cultured cortical neurons, findings that are compatible with the pronounced hyperpolarizing effect of latrepirdine on $\Delta\psi_p$. Latrepirdine's inhibition of glutamate-induced Ca^{2+} elevations and neuronal excitability is also of interest in the context of the failed clinical trials of latrepirdine in AD patients. While NMDA receptor hyperactivity has been suggested to be associated with AD, it is likewise accepted that sufficient NMDA receptor activity requires to be maintained to exert a beneficial effect in AD patients.[41]

While we observed a significant protective effect of prolonged latrepirdine pretreatment against glutamate excitotoxicity, acute pretreatment with latrepirdine failed to provide protection. Nor did acute pretreatment attenuate the glutamate-induced increase in cytosolic calcium, indicating that calcium influx may be the key signaling event that precipitates excitotoxic cell death. Prolonged pretreatment with latrepirdine activated AMPK, a kinase with both pro-survival,[10,42] but also cell death-inducing activities.[28] Our data demonstrate that there is a narrow range of latrepirdine concentrations that can exert a protective effect against excitotoxicity. This may reflect the moderate activation of AMPK within a pro-survival range, above which pro-death signaling occurs. We have recently shown that excessive or prolonged AMPK activation can lead to cell death through upregulation of pro-apoptotic BH3-only protein expression.[12,43,44] McCullough *et al*.[45] identified that continuous activation of AMPK increased neuronal injury during ischemia. Activation of AMPK has also been shown to potentiate neurodegeneration of striatal neurons in a mouse model of Huntington's disease.[46] On the other hand, AMPK activation has been shown to promote pro-survival signaling, and latrepirdine has recently been shown to stimulate autophagy and reduce the accumulation of α-synuclein *in vitro* and *in vivo*,[47] to enhance mTOR- and Atg5-dependent autophagy and to arrest progression of neuropathology in an AD mouse model.[48] Our data suggest that AMPK activation by latrepirdine may underlie the reported effects of latrepirdine on autophagy-mediated clearance of protein aggregates in such disease models. Indeed, induction of autophagy through AMPK-activating compounds has been shown before to enhance the clearance of both soluble and aggregated forms of Aβ and tau proteins *in vivo* and *in vitro*.[49] However, as AMPK may already be abnormally activated in symptomatic AD,[50] effects of AMPK activators such as latrepirdine on AD pathogenesis may strongly depend on disease progression. The experimental paradigm employed in our study naturally differs from the chronic exposure paradigm used in earlier clinical trials. Nevertheless, our *in vitro* data carefully argue for a potentially beneficial effect of latrepirdine in early AD, rather than at an advanced disease stage. Likewise, latrepirdine may be effective in individuals at risk of developing neurodegenerative disorders when given pre-symptomatically, for example, in familial forms of neurodegenerative disorders.

AMPK is considered a key sensor of the cellular energy status. AMPK signaling regulates energy balance at the cellular, organ and whole-body level.[10] Our findings that latrepirdine activates AMPK, and that the activation of AMPK by latrepirdine requires the upstream kinases LKB1 and CaMKKβ, shed new light into the mechanism of action of latrepirdine. Knockdown of either LKB1 or CaMKKbeta, the upstream kinases that activate AMPK, prevented the latrepirdine-induced increase in plasma membrane potential. This indicates latrepirdine may act upstream of both of these kinases to induce hyperpolarization. CaMKKbeta is thought to activate AMPK in response to increased levels of intracellular calcium concentration,[31] whereas LKB1 is required for maintaining baseline AMPK phosphorylation levels.[51] Although we show that latrepirdine reduced the amplitude of spontaneous calcium oscillations, we did not observe an increase in overall intracellular calcium *per se* on addition of latrepirdine. This suggests that the effects of latrepirdine on AMPK phosphorylation are independent of the effects on calcium. Thus, the activation of AMPK may result from latrepirdine activity at sites upstream of AMPK itself. In accordance with this hypothesis, treatment with latrepirdine progressively increased AMPK activity over 24 h, and hyperpolarization of $\Delta\psi_p$ also continued to occur for the duration of the 4-h experiment. However, treatment with latrepirdine immediately attenuated Ca^{2+} oscillations, indicating that latrepirdine has direct effects on proteins involved in neuronal Ca^{2+} dynamics. Therefore, further molecular and structural studies will be required to determine precise targets and binding sites. Nevertheless, the observation that 0.1 nM latrepirdine activates AMPK indicates that this compound is one of the most potent pharmacological activators of AMPK described so far.

CONFLICT OF INTEREST

The authors declare no conflict of interest.

ACKNOWLEDGMENTS

This research was supported by grants from Pfizer (Groton, CT, USA), Science Foundation Ireland (08/INV.1/B1949), the European Union FP7 Marie Curie OXY-SENSE IAPP program and the Higher Education Authority PRTLI Cycle 4 (National Biophotonics and Imaging Platform Ireland) to JHMP. PW is supported by the VIPS Program (funded by Austrian Federal Ministry of Science and Research and City of Vienna). TB was the recipient of a Marie Curie Co-fund CEMP fellowship. We thank Dr Andy Protter (Medivation, San Francisco, CA, USA) for advice and providing Latrepirdine, and Dr Gerhardt Boukes and Sarah Cannon for technical assistance.

REFERENCES

1 Giorgetti M, Gibbons JA, Bernales S, Alfaro IE, Drieu La Rochelle C, Cremers T *et al.* Cognition-enhancing properties of Dimebon in a rat novel object recognition task are unlikely to be associated with acetylcholinesterase inhibition or N-methyl-D-aspartate receptor antagonism. *J Pharmacol Exp Ther* 2010; **333**: 748–757.
2 Vignisse J, Steinbusch HW, Bolkunov A, Nunes J, Santos AI, Grandfils C *et al.* Dimebon enhances hippocampus-dependent learning in both appetitive and inhibitory memory tasks in mice. *Prog Neuropsychopharmacol Biol Psychiatry* 2011; **35**: 510–522.
3 Webster SJ, Wilson CA, Lee CH, Mohler EG, Terry Jr. AV, Buccafusco JJ. The acute effects of dimebolin, a potential Alzheimer's disease treatment, on working memory in rhesus monkeys. *Br J Pharmacol* 2011; **164**: 970–978.
4 Doody RS, Gavrilova SI, Sano M, Thomas RG, Aisen PS, Bachurin SO *et al.* Effect of dimebon on cognition, activities of daily living, behaviour, and global function in patients with mild-to-moderate Alzheimer's disease: a randomised, double-blind, placebo-controlled study. *Lancet* 2008; **372**: 207–215.
5 Zhang S, Hedskog L, Petersen CA, Winblad B, Ankarcrona M. Dimebon (latrepirdine) enhances mitochondrial function and protects neuronal cells from death. *J Alzheimers Dis* 2010; **21**: 389–402.
6 Moreira PI, Zhu X, Wang X, Lee HG, Nunomura A, Petersen RB *et al.* Mitochondria: a therapeutic target in neurodegeneration. *Biochim Biophys Acta* 2010; **1802**: 212–220.
7 Miller G. Pharmacology. The puzzling rise and fall of a dark-horse Alzheimer's drug. *Science* 2010; **327**: 1309.
8 Jones RW. Dimebon disappointment. *Alzheimers Res Ther* 2010; **2**: 25.
9 Naga KK, Geddes JW. Dimebon inhibits calcium-induced swelling of rat brain mitochondria but does not alter calcium retention or cytochrome C release. *Neuromolecular Med* 2011; **13**: 31–36.
10 Weisova P, Concannon CG, Devocelle M, Prehn JH, Ward MW. Regulation of glucose transporter 3 surface expression by the AMP-activated protein kinase mediates tolerance to glutamate excitation in neurons. *J Neurosci* 2009; **29**: 2997–3008.
11 Ward MW, Rego AC, Frenguelli BG, Nicholls DG. Mitochondrial membrane potential and glutamate excitotoxicity in cultured cerebellar granule cells. *J Neurosci* 2000; **20**: 7208–7219.
12 Concannon CG, Tuffy LP, Weisova P, Bonner HP, Davila D, Bonner C *et al.* AMP kinase-mediated activation of the BH3-only protein Bim couples energy depletion to stress-induced apoptosis. *J Cell Biol* 2010; **189**: 83–94.
13 Choi DW. Glutamate neurotoxicity and diseases of the nervous system. *Neuron* 1988; **1**: 623–634.
14 Rothman SM, Olney JW. Glutamate and the pathophysiology of hypoxic--ischemic brain damage. *Ann Neurol* 1986; **19**: 105–111.
15 Castellanos M, Sobrino T, Pedraza S, Moldes O, Pumar JM, Silva Y *et al.* High plasma glutamate concentrations are associated with infarct growth in acute ischemic stroke. *Neurology* 2008; **71**: 1862–1868.
16 Dong XX, Wang Y, Qin ZH. Molecular mechanisms of excitotoxicity and their relevance to pathogenesis of neurodegenerative diseases. *Acta Pharmacol Sin* 2009; **30**: 379–387.
17 Ward MW, Huber HJ, Weisova P, Dussmann H, Nicholls DG, Prehn JH. Mitochondrial and plasma membrane potential of cultured cerebellar neurons during glutamate-induced necrosis, apoptosis, and tolerance. *J Neurosci* 2007; **27**: 8238–8249.
18 Ward MW, Kushnareva Y, Greenwood S, Connolly CN. Cellular and subcellular calcium accumulation during glutamate-induced injury in cerebellar granule neurons. *J Neurochem* 2005; **92**: 1081–1090.
19 Ward MW, Rehm M, Duessmann H, Kacmar S, Concannon CG, Prehn JH. Real time single cell analysis of Bid cleavage and Bid translocation during caspase-dependent and neuronal caspase-independent apoptosis. *J Biol Chem* 2006; **281**: 5837–5844.
20 Concannon CG, Ward MW, Bonner HP, Kuroki K, Tuffy LP, Bonner CT *et al.* NMDA receptor-mediated excitotoxic neuronal apoptosis in vitro and in vivo occurs in an ER stress and PUMA independent manner. *J Neurochem* 2008; **105**: 891–903.
21 Bachurin SO, Shevtsova EP, Kireeva EG, Oxenkrug GF, Sablin SO. Mitochondria as a target for neurotoxins and neuroprotective agents. *Ann N Y Acad Sci* 2003; **993**: 334–344, discussion 345–349.
22 Eckert SH, Eckmann J, Renner K, Eckert GP, Leuner K, Muller WE. Dimebon ameliorates amyloid-beta induced impairments of mitochondrial form and function. *J Alzheimers Dis* 2012; **31**: 21–32.
23 Nicholls DG, Ward MW. Mitochondrial membrane potential and neuronal glutamate excitotoxicity: mortality and millivolts. *Trends Neurosci* 2000; **23**: 166–174.
24 Krohn AJ, Wahlbrink T, Prehn JH. Mitochondrial depolarization is not required for neuronal apoptosis. *J Neurosci* 1999; **19**: 7394–7404.
25 Dussmann H, Rehm M, Kogel D, Prehn JH. Outer mitochondrial membrane permeabilization during apoptosis triggers caspase-independent mitochondrial and caspase-dependent plasma membrane potential depolarization: a single-cell analysis. *J Cell Sci* 2003; **116**(Pt 3): 525–536.
26 Freedman JC, Novak TS. Optical measurement of membrane potential in cells, organelles, and vesicles. *Methods Enzymol* 1989; **172**: 102–122.
27 Weisova P, Anilkumar U, Ryan C, Concannon CG, Prehn JH, Ward W. 'Mild mitochondrial uncoupling' induced protection against neuronal excitotoxicity requires AMPK activity. *Biochim Biophys Acta* 2012; **1817**: 744–753.
28 Weisova P, Davila D, Tuffy LP, Ward MW, Concannon CG, Prehn JH. Role of 5′-adenosine monophosphate-activated protein kinase in cell survival and death responses in neurons. *Antioxid Redox Signal* 2011; **14**: 1863–1876.
29 Ikematsu N, Dallas ML, Ross FA, Lewis RW, Rafferty JN, David JA *et al.* Phosphorylation of the voltage-gated potassium channel Kv2.1 by AMP-activated protein kinase regulates membrane excitability. *Proc Natl Acad Sci USA* 2011; **108**: 18132–18137.
30 Hawley SA, Pan DA, Mustard KJ, Ross L, Bain J, Edelman AM *et al.* Calmodulin-dependent protein kinase kinase-beta is an alternative upstream kinase for AMP-activated protein kinase. *Cell Metab* 2005; **2**: 9–19.
31 Woods A, Dickerson K, Heath R, Hong SP, Momcilovic M, Johnstone SR *et al.* Ca2 + /calmodulin-dependent protein kinase kinase-beta acts upstream of AMP-activated protein kinase in mammalian cells. *Cell Metab* 2005; **2**: 21–33.
32 Woods A, Johnstone SR, Dickerson K, Leiper FC, Fryer LG, Neumann D *et al.* LKB1 is the upstream kinase in the AMP-activated protein kinase cascade. *Curr Biol* 2003; **13**: 2004–2008.
33 Zhou G, Myers R, Li Y, Chen Y, Shen X, Fenyk-Melody J *et al.* Role of AMP-activated protein kinase in mechanism of metformin action. *J Clin Invest* 2001; **108**: 1167–1174.
34 Kim J, Kundu M, Viollet B, Guan KL. AMPK and mTOR regulate autophagy through direct phosphorylation of Ulk1. *Nat Cell Biol* 2011; **13**: 132–141.
35 Choi DW. Ionic dependence of glutamate neurotoxicity. *J Neurosci* 1987; **7**: 369–379.
36 Ascher P, Nowak L. A patch-clamp study of excitatory amino acid activated channels. *Adv Exp Med Biol* 1986; **203**: 507–511.
37 Budd SL, Nicholls DG. Mitochondria, calcium regulation, and acute glutamate excitotoxicity in cultured cerebellar granule cells. *J Neurochem* 1996; **67**: 2282–2291.
38 Wang J, Ferruzzi MG, Varghese M, Qian X, Cheng A, Xie M *et al.* Preclinical study of dimebon on beta-amyloid-mediated neuropathology in Alzheimer's disease. *Mol Neurodegener* 2011; **6**: 7.
39 Day M, Chandran P, Luo F, Rustay NR, Markosyan S, LeBlond D *et al.* Latrepirdine increases cerebral glucose utilization in aged mice as measured by [18F]-fluorodeoxyglucose positron emission tomography. *Neuroscience* 2011; **189**: 299–304.
40 Howarth C, Gleeson P, Attwell D. Updated energy budgets for neural computation in the neocortex and cerebellum. *J Cereb Blood Flow Metab* 2012; **32**: 1222–1232.
41 Lipton SA. Pathologically-activated therapeutics for neuroprotection: mechanism of NMDA receptor block by memantine and S-nitrosylation. *Curr Drug Targets* 2007; **8**: 621–632.
42 Culmsee C, Monnig J, Kemp BE, Mattson MP. AMP-activated protein kinase is highly expressed in neurons in the developing rat brain and promotes neuronal survival following glucose deprivation. *J Mol Neurosci* 2001; **17**: 45–58.
43 Davila D, Connolly NM, Bonner H, Weisova P, Dussmann H, Concannon CG *et al.* Two-step activation of FOXO3 by AMPK generates a coherent feed-forward loop determining excitotoxic cell fate. *Cell Death Differ* 2012; **19**: 1677–1688.
44 Kilbride SM, Farrelly AM, Bonner C, Ward MW, Nyhan KC, Concannon CG *et al.* AMP-activated protein kinase mediates apoptosis in response to bioenergetic stress through activation of the pro-apoptotic Bcl-2 homology domain-3-only protein BMF. *J Biol Chem* 2010; **285**: 36199–36206.
45 McCullough LD, Zeng Z, Li H, Landree LE, McFadden J, Ronnett GV. Pharmacological inhibition of AMP-activated protein kinase provides neuroprotection in stroke. *J Biol Chem* 2005; **280**: 20493–20502.

46 Ju TC, Chen HM, Lin JT, Chang CP, Chang WC, Kang JJ *et al.* Nuclear translocation of AMPK-alpha1 potentiates striatal neurodegeneration in Huntington's disease. *J Cell Biol* 2011; **194**: 209–227.
47 Steele JW, Ju S, Lachenmayer ML, Liken J, Stock A, Kim SH *et al.* Latrepirdine stimulates autophagy and reduces accumulation of alpha-synuclein in cells and in mouse brain. *Mol Psychiatry* 2013; **18**: 882–888.
48 Steele JW, Lachenmayer ML, Ju S, Stock A, Liken J, Kim SH *et al.* Latrepirdine improves cognition and arrests progression of neuropathology in an Alzheimer's mouse model. *Mol Psychiatry* 2013; **18**: 889–897.
49 Wang Y, Martinez-Vicente M, Kruger U, Kaushik S, Wong E, Mandelkow EM *et al.* Tau fragmentation, aggregation and clearance: the dual role of lysosomal processing. *Hum Mol Genet* 2009; **18**: 4153–4170.
50 Vingtdeux V, Davies P, Dickson DW, Marambaud P. AMPK is abnormally activated in tangle- and pre-tangle-bearing neurons in Alzheimer's disease and other tauopathies. *Acta Neuropathol* **121**: 337–349.
51 Shaw RJ, Kosmatka M, Bardeesy N, Hurley RL, Witters LA, DePinho RA *et al.* The tumor suppressor LKB1 kinase directly activates AMP-activated kinase and regulates apoptosis in response to energy stress. *Proc Natl Acad Sci USA* 2004; **101**: 3329–3335.

Supplementary Information accompanies the paper on the Translational Psychiatry website (http://www.nature.com/tp)